Bullet Groups in the Bolshoi Cosmological Simulation

J. G. Fernández-Trincado[1,2,3], J. E. Forero-Romero[1] and T. Vergudo[3]

[1] *Departamento de Física, Universidad de los Andes, Cra. 1 No. 18A-10, Edificio Ip, Bogotá, Colombia*

[2] *Institute Utinam, CNRS UMR6213, Université de Franche-Comté, OSU THETA de Franche-Comté-Bourgogne, Besançon, France*

[3] *Centro de Investigaciones de Astronomía, AP 264, Mérida 5101-A, Venezuela*

ABSTRACT

We estimate the expected distribution of displacements between the host halo of dark matter and the substructure of dark matter most massive of the host, using a halo catalog from the Bolshoi simulation detected with the Bound Density Maximun (BDM) algorithm. We found that the probability of finding a system similar to the Bullet Group with displacements of $\sim$400 kpch^{-1} is between 40% for z= 0 and 60% for z= 1 and ΛCDM standard model predicts this scenario and is consistent with recently observations of the object SL2S J08544-0121 that is a gravitational lens found in the SL2S and located at z= 0.35.

1. Introduction

This paper is organized as the follows: In Section 2 we present the simulations.

2. Simulation

The analysis presented in this paper uses mainly the Bolshoi (250 Mpch^{-1} simulation box, 1 kpch^{-1} resolution) Database simulation described in Klypin et al. (2011). The simulation follows the evolution of 8.6 billion particle cosmological N-body simulation from z=80 to z=0 in a comoving cube of 250 Mpch^{-1} on a side. The cosmology used corresponds to the spatially flat concordance model with the following parameters: the density parameter for matter (dark matter+baryons) $\Omega_m = 0.27$, the density parameter for baryonic matter $\Omega_b = 0.0469$, the density parameter for dark energy $\Omega_\Lambda = 0.73$, the Hubble parameter $h = 0.7$, the normalization of the Power spectrum $n = 0.95$ and the amplitude of mass density fluctuation (at redshift z=0) $\sigma_8 = 0.82$. The number of particles used for each of the DM component was 2048^3, resulting in a mass resolution of 1.35×10^8 M$_\odot$h^{-1}.

3. Cumulative Probability Distributions

We selected four snapshot of the simulation for four different redshifts (z= 0, z= 0.25, z= 0.5 and z= 1) based in the distribution of redshift in the Figure 1 by Verdugo et al. (2014), and for each sample in redshift we selected the host halo with circular velocities greater than 300 kms^{-1} and was split in two principal groups: The first group correspond to host halo with circular velocities between 300 kms^{-1} to 700 kms^{-1} with mass in the range of 10^{12} M$_\odot$ to 10^{14} M$_\odot$ in the range of mass of the Bullet Groups, and second group correspond to host halo with circular velocities greater than 700 kms^{-1} with mass $\geq 10^{14}$ M$_\odot$, in the range of mass of the Bullet Clusters, in the Table 1 is shown the two groups selected in this work. For each group, we classified the corresponding substructures most massive and associated with the corresponding host halo. The configuration of this system is shown in Figure 1, where you can distinguish the host halo and substructure for a particular configuration in z= 0. In this work, we estimate the expected distribution of displacements ($d_{real,(X,Y)}$) in the projection 2-D that can estimate by observations, these displacements correspond to the separation between the minimal potential of the host halo and the minimal potential of the substructure, both are dark matter distributions.

In order to explore the distribution of displacements expected in the observational, we define a new parameter given by:

$$\frac{\nu_{circ,sub}}{\nu_{circ,halo}} = 0.5 \tag{1}$$

Figure 2 shows the scatter plot of the parameter $\left(\frac{\nu_{circ,sub}}{\nu_{circ,halo}}\right)$ vs the displacement ($d_{2d,(X,Y)}$) between the host halo and the substructure and for different redshifts. This parameter is consistent with the observations. The red star simbol in the Figure 2 is equal to 0.54 corresponding to the fraction in velocity dispersion in the line-of-sigth of the group SL2S SJ08544-0121 ($\sigma_{host,halo} = 341^{+43}_{-109}$ kms^{-1} and $\sigma_{substructure} = 185^{+30}_{-62}$), reported by Muñoz

Sample	Minimum Mass M$_\odot$h^{-1}	Maximum Mass M$_\odot$h^{-1}	# Halos $z = 0$	# Halos $z = 0.25$	# Halos $z = 0.5$	# Halos $z = 1$
Host Halo	0.35×10^{14}	1.09×10^{14}	400	362	310	192
Substructure	0.38×10^{11}	0.30×10^{14}	400	362	310	192

Table 1: Mass ranges for the two groups selected in this work in different redshifts.

et al. (2013). Based in the parameter $\left(\frac{\nu_{circ,sub}}{\nu_{circ,halo}}\right) > 0.5$, we estimate the expected distribution of displacements and this is shown in the Figure 3 for the two groups classified in this work.

3.1. Number expected of Bullet Groups in the sample

In order of estimate the number of Bullet Groups expected in the Bolshoi Cosmological Simulation, we define the configuration of this system as one where the substructure is coming out of the host halo ($cos(\theta) > 0.5$). For this we make the scalar product between the velocity vector and position vector that defines the separation between the host halo and the substructure, as shown below:

$$cos(\theta) = \frac{\vec{\nu} \cdot \vec{r}}{\|\nu\| \, \|r\|} \tag{2}$$

where, $\vec{\nu} = \vec{\nu}_{sub} - \vec{\nu}_{halo}$ and $\vec{r} = \vec{r}_{sub} - \vec{r}_{halo}$, in the Figure 4 is shown the scatter plot of $cos(\theta)$ vs $X_{off,new} = \frac{d_{2d,(X,Y)}}{R_{virial,halo}} = \frac{d_{real,(X,Y)}}{R_{virial,halo}}$.

4. Summary

5. Conclusions

Acknowledgements

The CosmoSim database used in this paper is a service by the Leibniz-Institute for Astrophysics Potsdam (AIP). The BolshoiP simulation was performed within the Bolshoi project of the University of California High-Performance AstroComputing Center (UC-HIPACC) and was run at the NASA Ames Research Center.

REFERENCES

Klypin, A. A. and Trujillo-Gomez, S. and Primack, J. 2011, ApJ, 102

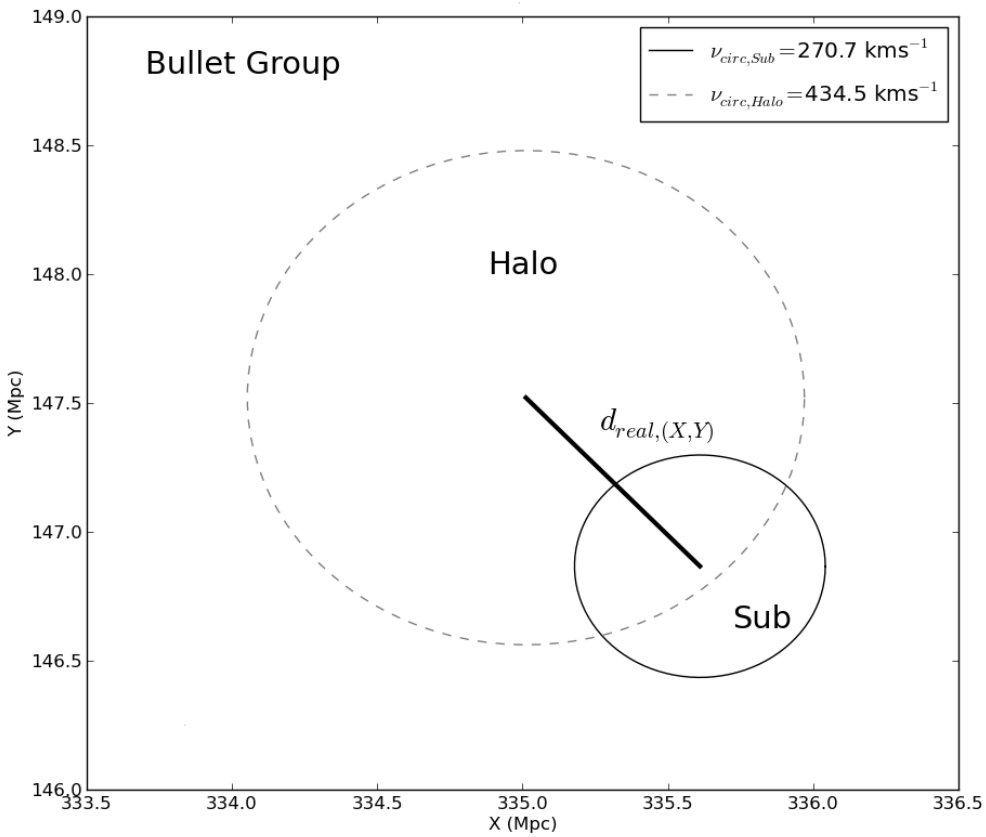

Fig. 1.— Configuration for a host halo (dashed circle) and sub-structure (black circle) in the sample.

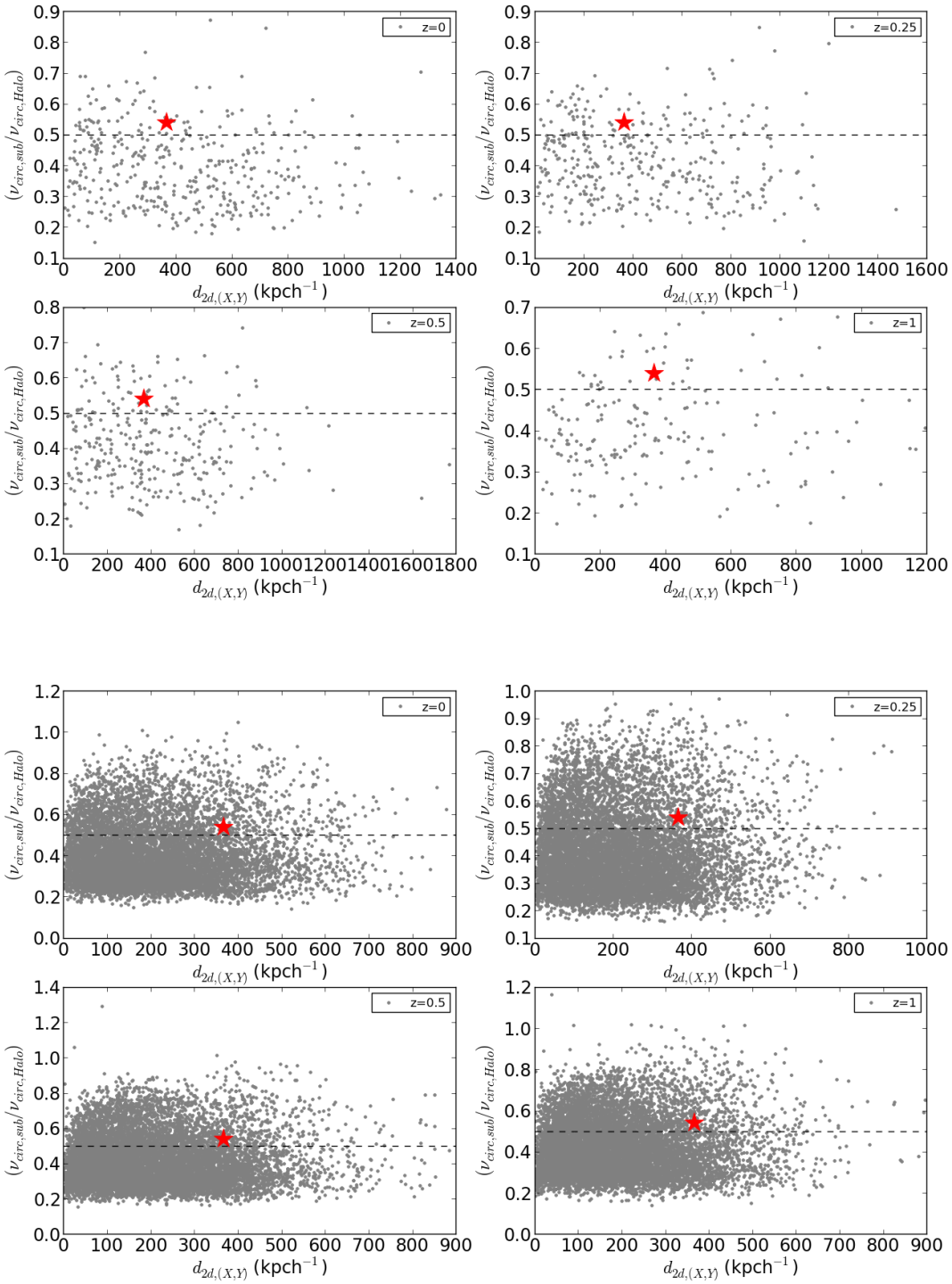

Fig. 2.— Scatter $\left(\frac{\nu_{circ,sub}}{\nu_{circ,halo}}\right)$ vs $d_{2d,(X,Y)}$ for different redshifts. The horizontal dashed line correpond to $\left(\frac{\nu_{circ,sub}}{\nu_{circ,halo}}\right) = 0.5$ and the red star simbol correspond to $\left(\frac{\nu_{circ,sub}}{\nu_{circ,halo}}\right) = 0.54$ for SL2S SJ08544-0121 in Muñoz et al. (2013). The four top panels are the sample with circular velocities > 700 kms^{-1} and the four down panels are the sample with circular velocities between 300 km s^{-1} to 700 kms^{-1}.

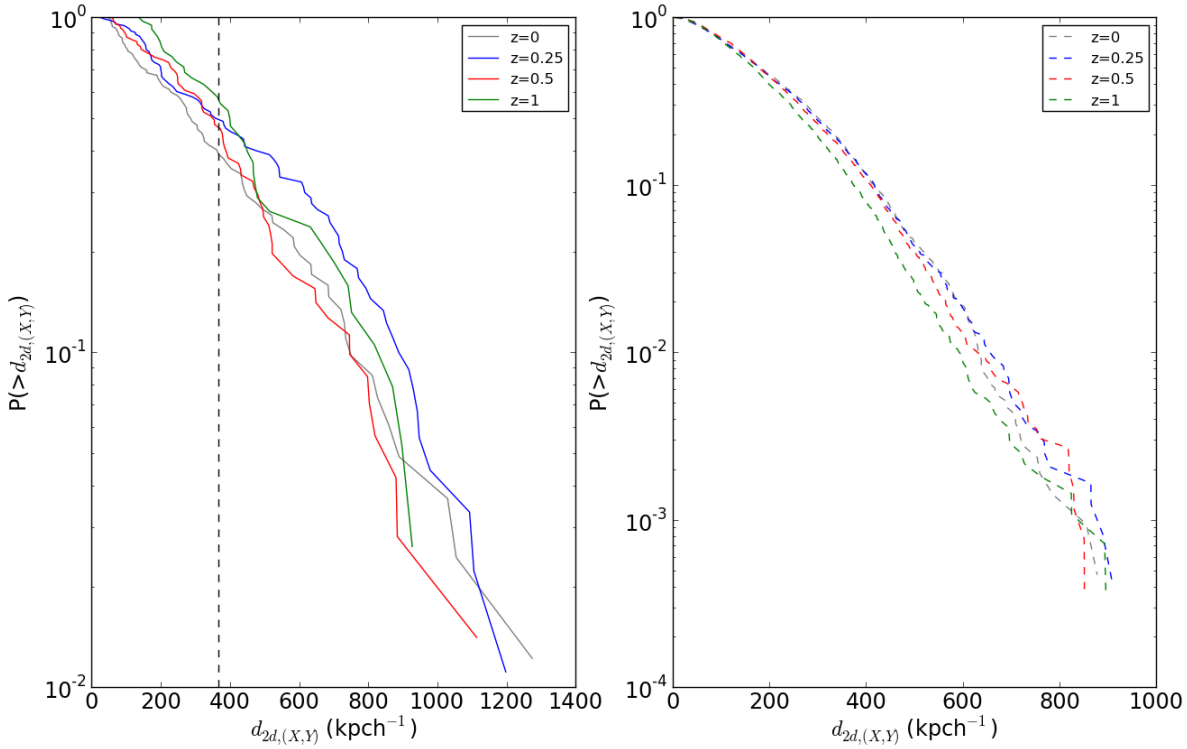

Fig. 3.— Cumulative distribution (P> $d_{2d,(X,Y)}$) of displacements for the projection (X,Y). **Left panel:** Sample with $\nu_{max} > 700$ kms^{-1} for different redshifts. The vertical dashed line, correspond to the separation between dark matter to dark matter estimate in this work as the double of separation between the collisional gas and dark matter of 124±20 kpc reported by Gastaldello et al. (2014) for the group SL2S J08544-0121. **Right panel:** Sample with 300 kms^{-1} $< \nu_{max} <$ 700 kms^{-1} for different redshifts.

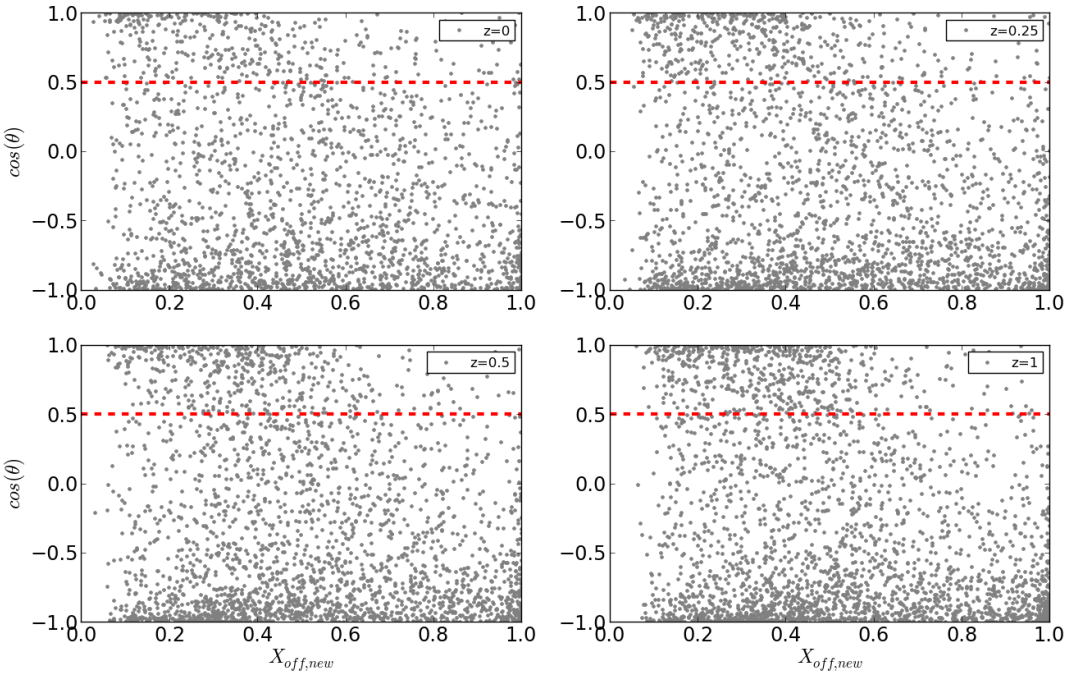

Fig. 4.— Scatter of $cos(\theta)$ vs $X_{off,new}$. The red dashed line correpond to the limit for $cos(\theta) > 0.5$, where the substructure is emerging from the host halo and $\left(\frac{\nu_{circ,sub}}{\nu_{circ,halo}}\right) \geq 0.5$, cicular velocities < 700 kms^{-1} and different redshifts.

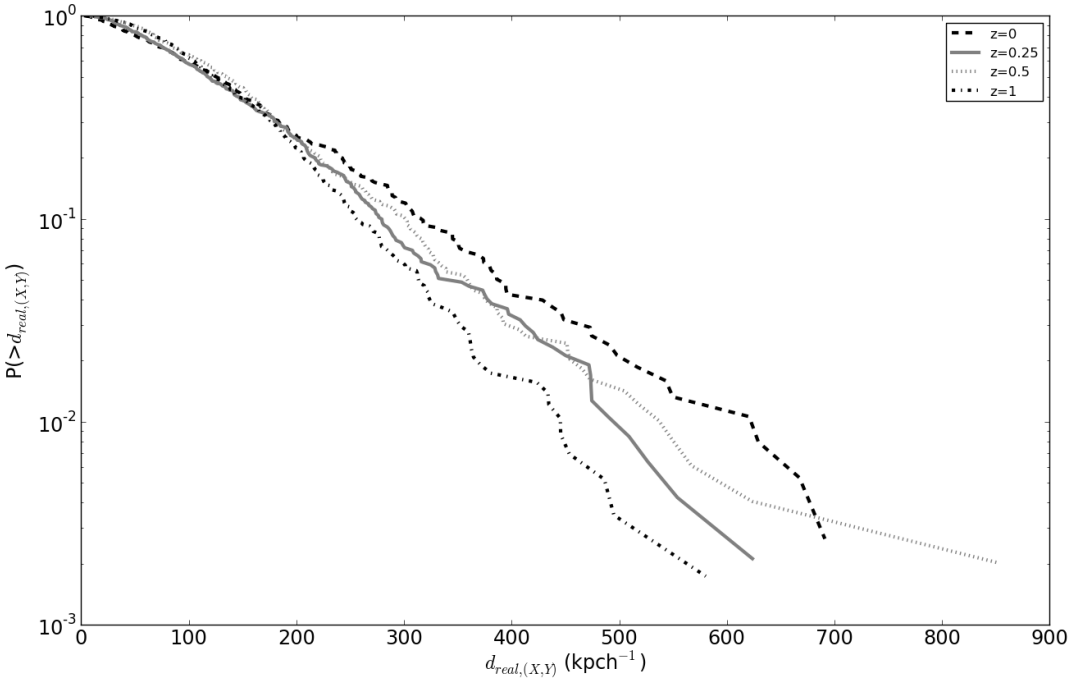

Fig. 5.— Cumulative distribution of $d_{real,(X,Y)}$ for $cos(\theta) > 0.5$, $\left(\frac{\nu_{circ,sub}}{\nu_{circ,halo}}\right) \geq 0.5$, cicular velocities < 700 kms^{-1} and different redshifts.

Vedugo, T., Motta, V., Foex, G., Forero-Romero, J. E., Muñoz, R. P., Pello, R., Limousin, M., Gavazzi, R., More, A., Cabanac, R., Soucail, G., Blakeslee, J. P., Mejía, A., Magris, G. and Fernández-Trincado, J. G. 2014, ApJ, in preparation

Gastaldello, F., et al. 2014, MNRAS, in preparation

Muñoz, R. P. and Motta, V. and Verdugo, T. and Garrido, F. and Limousin, M. and Padilla, N. and Foëx, G. and Cabanac, R. and Gavazzi, R. and Barrientos, L. F. and Richard, J. 2013, A&A, A80